High-pressure elastic properties of the VI and VII phase of ice in dense H_2O and D_2O

H. Shimizu, T. Nabetani, T. Nishiba, and S. Sasaki
Department of Electronics and Computer Engineering, Gifu University, 1-1 Yanagido, Gifu 501-11, Japan
(Received 29 September 1995; revised manuscript received 16 November 1995)

High-pressure Brillouin spectroscopy has been used to determine acoustic velocities in any direction, refractive index, adiabatic elastic constants, and adiabatic bulk modulus of H_2O and D_2O ices at 300 K and at pressures between 1.05 and 2.1 GPa for tetragonal ice VI and above pressures up to 8 GPa for cubic ice VII. Typical values of elastic constants for H_2O ice VI are $C_{11}=32.8$, $C_{12}=11.8$, $C_{13}=14.7$, $C_{33}=27.8$, $C_{44}=6.3$, and $C_{66}=5.9$ GPa at the pressure of 1.23 GPa. Refractive index and elastic constants show no distinction between H_2O and D_2O over the observed pressure ranges. At ice VI→VII transition at 2.1 GPa, acoustic velocities, refractive index, and elastic constants present drastic changes, but the adiabatic bulk modulus shows almost continuous change which is most likely to relate the common features of the self-clathrate structure and the potential function in both VI and VII ices.

I. INTRODUCTION

The H_2O ice shows about ten phases under different conditions of pressure and temperature.[1] An interesting variety of these polymorphisms is mainly due to the hydrogen bond and the structural versatility of H_2O molecules. These features of H_2O ices at high pressures have been attracting attention in condensed matter and planetary science. High-pressure Brillouin spectroscopy is a useful method to study the elastic properties of molecular single crystals grown in a diamond anvil cell (DAC):[2–4] Acoustic velocities (v) for any direction, the refractive index (n), the polarizability (α), adiabatic elastic constants (C_{ij}), and adiabatic bulk modulus (B_s) can be exactly determined by Brillouin scattering measurements with *in situ* identification of the crystal orientation at each pressure by analyzing the observed angular dependence of acoustic velocities. These results provide some insight into the forces of interaction between atoms and, in particular, into the disruption of these forces.

At room temperature, compression of liquid water leads to a tetragonal ice VI at pressures above 1.05 GPa ($a=6.18$ Å and $c=5.70$ Å at $T=225$ K) and further to a cubic ice VII above 2.1 GPa ($a=3.34$ Å at $T=295$ K). The structures of ices VI and VII can be built up from two interpenetrated but unconnected zeolitelike and diamond-type sublattices of oxygen atoms, respectively.[5] In these high-pressure ices, high density is achieved by forming this "self-clathrate" structure.[6] The intuitive view of the ice-VI structure is shown in Fig. 1. Each H_2O molecule (represented by a ball) has four nearest neighbors and is hydrogen bonded to these (protons are disordered). The four neighbors form a rather highly distorted tetrahedron around the central H_2O molecule. Hydrogen-bonded chains are linked to form an open zeolitelike sublattice. The cavities of one sublattice accommodate the chains of the second sublattice. The structure of the ice VII formed by two diamond-type sublattices was presented in our recent publication.[7]

Polian and Grimsditch[8–10] measured the Brillouin spectra only at a scattering geometry of 180° and observed the pressure dependence of nv in ices VI and VII without identification of the crystal orientation. From the pressure dependence of nv, they observed the VI→VII phase transition at about 2.1 GPa. Very recently, we have determined sound velocities for all directions and three elastic constants (C_{11}, C_{12}, and C_{44}) of cubic H_2O ice VII under pressures between 2.1 and 8 GPa at 300 K by Brillouin measurements[7] and have found the unusual result that the Cauchy relation ($C_{12}=C_{44}$) holds at every pressure. This result suggests that the interactions between the atoms can be described by central forces.

In this paper, we present acoustic velocities for any direction, the refractive index, and six elastic constants (C_{11}, C_{12}, C_{13}, C_{33}, C_{44}, and C_{66}) of H_2O and D_2O ices VI under pressures between 1.05 and 2.1 GPa at 300 K with *in situ* identification of its single-crystal orientation. From these results and the present D_2O ice VII, including our recent re-

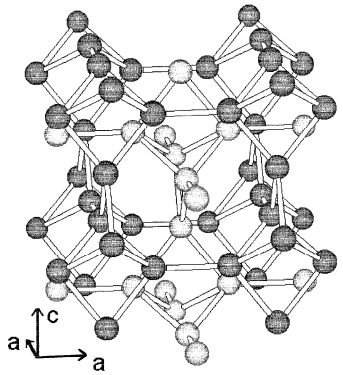

FIG. 1. Tetragonal ice-VI structure. Oxygen atoms of H_2O molecules are represented by balls, and hydrogen bonds linking the molecules are shown as sticks (protons are disordered, and the hydrogen atoms are not shown). Each H_2O molecule has four nearest neighbors and is hydrogen bonded to these. The four neighbors form a rather highly distorted tetrahedron around the central H_2O molecule. The H_2O molecules are linked by the hydrogen bonds to form chains parallel to the a axes, so as to form an open zeolitelike sublattice. These two sublattices, distinguished by fully and partially shaded atoms, interpenetrate but do not interconnect (self-clathrate). The cavities of one sublattice accommodate the chains of the second sublattice.

sults for H_2O ice VII,[7] we investigate the characteristics of elastic properties for ice VI→VII phase transition at $P=2.1$ GPa.

II. THEORETICAL BASICS

From the Brillouin equation for the tetragonal system,[11] we can express the square of sound velocity v_j as a function of nine parameters,

$$v_j^2=g_j(C_{11}/\rho,C_{12}/\rho,C_{13}/\rho,C_{33}/\rho,C_{44}/\rho,C_{66}/\rho,\theta,\phi,\chi), \tag{1}$$

where the subscript j (=0,1,2) indicates LA, TA_1 (slow), and TA_2 (fast) modes, respectively, ρ is the density, and the Euler angles (θ,ϕ,χ) relate the laboratory frame (X,Y,Z) to the crystal reference frame (x,y,z). In order to determine three Euler angles and six elastic constants at each pressure, we applied a computerized least-squares fit between calculations $g_j(\phi_i)$ and experimental velocities (ϕ_i,v_{ji}) as a function of angle ϕ_i,

$$J=\sum_{ij}\,[g_j(\phi_i)-v_{ji}]^2, \quad j=0,1,2, \tag{2}$$

where J is minimized by systematically varying the nine parameters until the fit is optimized. As a result, we can determine the crystal orientation (θ,ϕ,χ) and acoustic velocities for arbitrary directions. In a later part, we will investigate the anisotropic degree of the refractive index and its effect on the acoustic velocities in the ice-VI phase.

III. EXPERIMENT

A single crystal of ice VI was grown by increasing the pressure on a seed crystal, which coexists with the water at about 1.05 GPa and 300 K in a DAC. The shape of the seed crystal was usually observed under the microscope. Therefore we can estimate approximately the orientation of the crystal filled in the entire DAC chamber on the basis of Yamamoto's x-ray study for crystal facets.[12] Ice VII in a DAC is usually polycrystalline, because it is produced through the phase transition of VI→VII at 300 K.[8] In order to grow a single crystal of ice VII, we used a new route through the direct phase transition of water→ice VII above the triple point ($P=2.2$ GPa, $T=355$ K) of liquid and ice VI and VII phases.[7] We succeeded to grow a single crystal of ice VII, but the crystal facets could not be observed.

A Sandercock tandem Fabry-Pérot interferometer[13] was used in the triple-pass arrangement[14] for Brillouin scattering measurements.[15,16] The 514.5-nm argon-ion laser line (λ_0), providing a single-moded power of about 100 mW, was used as the excitation source. The Brillouin frequency shifts ($\Delta\nu$) at 60°, 90°, and 180° (angles between the incident and the scattered beams) scattering geometries with the DAC are related to the acoustic velocity (v) as follows:[17]

$$\Delta\nu_{60}=v_{60}/\lambda_0, \tag{3}$$

$$\Delta\nu_{90}=\sqrt{2}v_{90}/\lambda_0, \tag{4}$$

and

$$\Delta\nu_{180}=(2n)v_{180}/\lambda_0, \tag{5}$$

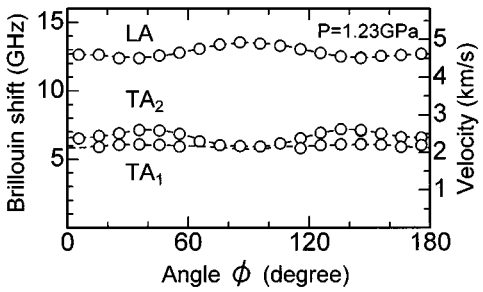

FIG. 2. Brillouin frequency shifts and acoustic velocities of LA, TA_2, and TA_1 modes as a function of angle ϕ at a 90° scattering geometry for H_2O ice VI at $P=1.23$ GPa. Open circles indicate experimental points, and the dashed lines represent the calculated best-fit velocities.

where the wave vector $\boldsymbol{q}$ of probed acoustic phonons is parallel (60° and 90°) and perpendicular (180°) to interfaces of the input and output diamonds crossed by the laser beam, and v_{60} and v_{90} are independent of the refractive index of the medium.

IV. RESULT AND DISCUSSION

A. Ice VI

For ice VI Brillouin measurements were made at 90° scattering geometry in 10° intervals of the rotation angle ϕ about the load axis of the DAC. The observed Brillouin shifts, that is, sound velocities for H_2O ice at 1.23 GPa [from Eq. (4)], are plotted as a function of ϕ by open circles in Fig. 2. To analyze the angular dependence of velocities of the LA and the two TA_1 (slow) and TA_2 (fast) modes at each applied pressure, we used Eq. (1). The computerized least-squares fit was applied to determine the elastic constants and Euler angles (orientation of a H_2O single crystal grown in the DAC). The best-fit calculations are represented by the dashed lines in Fig. 2. To support the determination of Euler angles, we made the visual observation of crystal facets for a ice-VI single crystal[12] grown in the DAC under microscope. There is excellent agreement between the measured and fitted values, which yielded for H_2O VI at 1.23 GPa, $C_{11}/\rho=23.1$ km^2 s^{-2}, $C_{12}/\rho=8.3$ km^2 s^{-2}, $C_{13}/\rho=10.4$ km^2 s^{-2}, $C_{33}/\rho=19.6$ km^2 s^{-2}, $C_{44}/\rho=4.4$ km^2 s^{-2}, and $C_{66}/\rho=4.2$ km^2 s^{-2} and the crystal orientation $\theta=44.7°$ and $\chi=0.78°$ within an accuracy of ±2%.

Once the nine parameters were determined, the acoustic velocities $[v=(C_{ij}/\rho)^{1/2}]$ could be calculated for all directions. Since the ice VI has a tetragonal cell, the ice-VI crystal is usually birefringent. In order to estimate the anisotropic degree of refractive index for tetragonal ice VI, we measured the angular dependence of $\Delta\nu_{180}$ at 180° scattering geometry [see Eq. (5)]. Since the velocity v_{180} is independent of the rotation (ϕ) along the load axis of the DAC, we can estimate the direction dependence of n by rotating the incident-light polarization (i.e., rotation of the DAC in 10° intervals). The ϕ dependence of $\Delta\nu_{180}$ for the LA mode was measured at $P=1.97$ GPa. The $\Delta\nu_{180}$ is almost independent of ϕ, that is, $\Delta\nu_{180}=26.85\pm0.135$ GHz. This result indicates that the birefringence is less than about 1%, which agrees with the previous study[8] by measuring Brillouin shifts with two cases

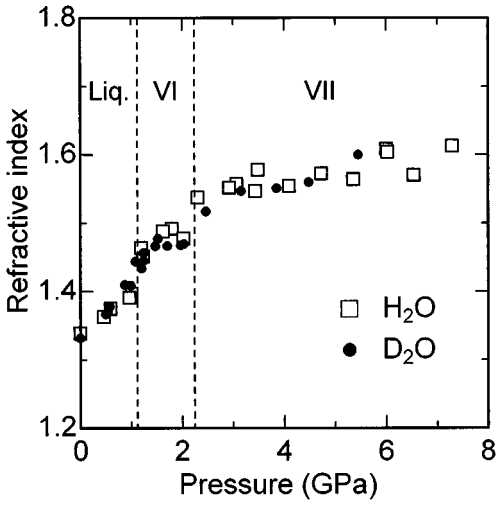

FIG. 3. Pressure dependence of refractive index at 300 K in liquid water up to 1.05 GPa, tetragonal ice VI up to 2.1 GPa, and cubic ice VII. Open squares indicate H_2O and solid circles D_2O.

of the incident light polarized parallel and perpendicular to the crystal axes at 180° scattering geometry. Therefore, from our analysis of sound velocity, we can neglect the anisotropy of the refractive index in the ice VI within the experimental error on the measurement of Brillouin frequency shifts. At the solidification point (=1.05 GPa), the sound velocity in a liquid shows discontinuous changes to LA, TA_2, and TA_1 in ice VI, and they increase with pressure. The distinction in acoustic velocities for H_2O ice (v_{H_2O}) and D_2O ice (v_{D_2O}) is understood by the kinetic theory, $v_{H_2O}/v_{D_2O}=(M_{D_2O}/M_{H_2O})^{1/2}=1.054$, where M_{D_2O} and M_{H_2O} are the molecular weights of D_2O and H_2O, respectively. This relation is approximately obeyed at each pressure.

Furthermore, we can calculate the acoustic velocity (v_{180}) along the direction perpendicular to the diamond interfaces, which is available to determine the refractive index (n) by using Eq. (5). From the $\Delta\nu_{180}$ measured at 180° scattering geometry, we can obtain the pressure dependence of n for H_2O and D_2O ice VI as shown in Fig. 3. The uncertainties in the measured frequency shifts and in the determined refractive index are about $\Delta(\Delta\nu)/\Delta\nu=\pm1\%$ and $\Delta n/n=\pm2\%$, respectively. At the freezing point, n shows a discontinuous increase of about 4% and, moreover, increases gradually with pressure up to $n=1.48$ at $P=2.1$ GPa. The n of H_2O ice shows almost the same values as D_2O ice, and the present results are in good agreement with those estimated by Polian and Grimsditch.[8]

In Fig. 4 we show a presentation of six elastic constants for H_2O ice VI as a function of pressure between 1.05 and 2.1 GPa by using the pressure dependence of ρ from x-ray studies.[18] Typical values at $P=1.23$ GPa are as follows: $C_{11}=32.8\pm0.66$ GPa, $C_{33}=27.8\pm0.56$ GPa, $C_{13}=14.7\pm0.29$ GPa, $C_{12}=11.8\pm0.24$ GPa, $C_{44}=6.3\pm0.13$ GPa, and $C_{66}=5.9\pm0.12$ GPa in the order of largeness. The Cauchy relation of $C_{12}=C_{66}$ and $C_{13}=C_{44}$ in a tetragonal system[19] does not hold at every pressure, which is a contrast to the atomic feature of central forces (=Cauchy relation) in the cubic ice VII.[7] This difference between VI and VII phases for interacting forces will be due to their zeolitelike and

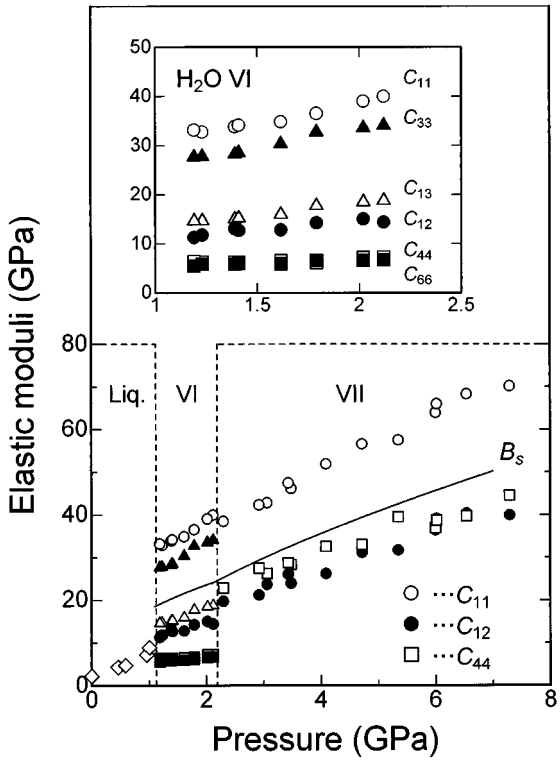

FIG. 4. Pressure dependence of elastic moduli in a liquid H_2O ($C=\rho v^2$) up to 1.05 GPa, tetragonal H_2O ice VI (C_{11}, C_{12}, C_{13}, C_{33}, C_{44}, and C_{66}) up to 2.1 GPa, and cubic H_2O ice VII (C_{11}, C_{12}, and C_{44}) at 300 K. The solid line indicates the adiabatic bulk modulus (B_s) in VI and VII ices.

diamond-type structures of the interpenetrating sublattices, respectively. Since both the molecular and hydrogen bonding geometries are less near perfection and more dispersed for VI than for VII, Kuhs *et al.*[20] suggest that the interaction between the independent sublattices is certainly different in VI and VII phases.

B. Ice VI→ice VII

For the cubic H_2O ice VII, we reported the pressure dependence of acoustic velocities and three adiabatic elastic constants at pressures from 2.1 to 8 GPa.[7] Here we investigate the characteristic change of elastic properties at the ice VI→VII phase transition by adding the refractive index and adiabatic bulk modulus of H_2O ice VII, and the present results of elastic properties for D_2O ice VII up to 6 GPa. The adiabatic bulk modulus (B_s) was calculated from the following for tetragonal ice VI and cubic ice VII, respectively:[21]

$$B_s=\frac{C_{33}C_{11}-2C_{13}^2+C_{33}C_{12}}{C_{11}+2C_{33}-4C_{13}+C_{12}}, \tag{6}$$

$$B_s=(C_{11}+2C_{12})/3. \tag{7}$$

The present results of B_s indicated by solid line in Fig. 4 are in reasonable agreement with the isothermal bulk modulus in ice VII studied by x-ray measurements[18] and a recent universal investigation.[22]

Acoustic velocities, the refractive index, and elastic constants increase with increasing pressure in liquid water, te-

tragonal ice VI, and cubic ice VII. Transition pressures of liquid→VI and VI→VII are almost the same for H_2O and D_2O ices. We can find, as expected, that acoustic velocities and elastic constants show drastic changes at the ice VI→VII transition point. However, it is noted that adiabatic bulk modulus (B_s) indicated by the solid line in Fig. 4 shows a continuous change at this point. This result is most likely to relate (1) the common feature of the ''self-clathrate'' structure in both VI and VII ices and (2) similar potential functions at their present experimental range.

Figure 5 shows the pressure dependence of elastic constants in H_2O and D_2O VII ices. The values of C_{11}, C_{12}, and C_{44} for D_2O ice VII are almost the same at each pressure as those reported previously for H_2O ice VII,[7] and the Cauchy relation ($C_{12}=C_{44}$) also holds for D_2O ice. Therefore we have not found the difference in elastic constants, refractive index, and transition pressures ($P_{\text{liquid}\rightarrow\text{VI}}$ and $P_{\text{VI}\rightarrow\text{VII}}$) for H_2O and D_2O within experimental errors, but confirmed the reasonable decrease in acoustic velocities for D_2O ice.

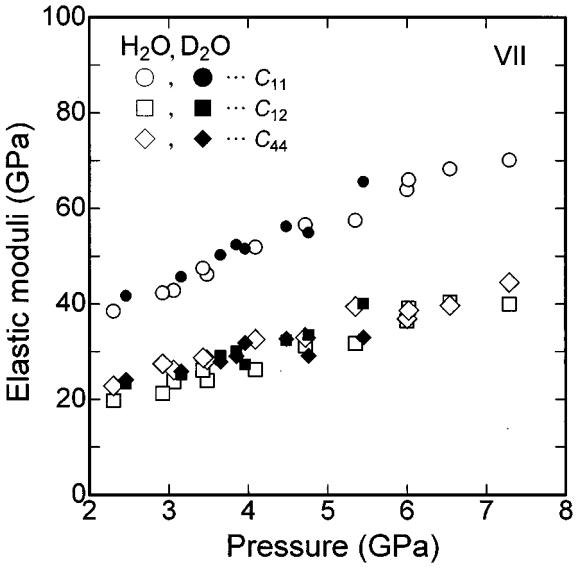

FIG. 5. Pressure dependence of elastic constants in cubic ice VII (C_{11}, C_{12}, and C_{44}) at 300 K. Open symbols indicate H_2O ice and solid symbols D_2O ice.

V. SUMMARY

Acoustic velocities in any direction, refractive index, adiabatic elastic constants, and adiabatic bulk modulus of H_2O and D_2O ices at 300 K have been determined at pressures between 1.05 and 2.1 GPa for tetragonal ice VI and above pressures up to 8 GPa for cubic ice VII by applying Brillouin spectroscopy whereby the crystal orientation in a DAC could be found in the same fitting analysis. The distinction in transition pressures, refractive index, and elastic constants between H_2O and D_2O has not been found in VI and VII ices. The Cauchy relation in tetragonal ice VI does not hold at every pressure, which is a contrast to that in cubic ice VII. From our experimental results, we investigated the characteristics of elastic properties for the ice VI→VII phase transition at $P=2.1$ GPa.

[1] V. P. Dmitriev, S. B. Rochal, and P. Toledano, Phys. Rev. Lett. **71**, 553 (1993).
[2] H. Shimizu and S. Sasaki, Science **257**, 514 (1992).
[3] H. Shimizu, T. Kitagawa, and S. Sasaki, Phys. Rev. B **47**, 11 567 (1993).
[4] H. Shimizu, H. Sakoh, and S. Sasaki, J. Phys. Chem. **98**, 670 (1994).
[5] B. Kamb, Science **150**, 205 (1965).
[6] J. P. Poirier, Nature (London) **299**, 683 (1982).
[7] H. Shimizu, M. Ohnishi, S. Sasaki, and Y. Ishibashi, Phys. Rev. Lett. **74**, 2820 (1995).
[8] A. Polian and M. Grimsditch, Phys. Rev. B **27**, 6409 (1983).
[9] A. Polian and M. Grimsditch, Phys. Rev. Lett. **52**, 1312 (1984).
[10] A. Polian and M. Grimsditch, Phys. Rev. B **29**, 6362 (1984).
[11] A. G. Every, Phys. Rev. B **22**, 1746 (1980).
[12] K. Yamamoto, Jpn. J. Appl. Phys. **21**, 803 (1982).
[13] R. Mock, B. Hillebrands, and R. Sandercock, J. Phys. E **20**, 656 (1987).
[14] H. Shimizu, N. Nakashima, and S. Sasaki, Phys. Rev. B **53**, 111 (1996).
[15] A. K. Ramdas, S. Rodriguez, M. Grimsditch, T. R. Anthony, and W. F. Banholzer, Phys. Rev. Lett. **71**, 189 (1993).
[16] M. Grimsditch, E. S. Zouboulis, and A. Polian, J. Appl. Phys. **76**, 832 (1994).
[17] H. Shimizu, E. M. Brody, H. K. Mao, and P. M. Bell, Phys. Rev. Lett. **47**, 128 (1981).
[18] R. G. Munro, S. Block, F. A. Mauer, and G. Piermarini, J. Appl. Phys. **53**, 6174 (1982).
[19] M. Born and K. Huang, *Dynamical Theory of Crystal Lattices* (Oxford University Press, Oxford, 1985), p. 136.
[20] W. F. Kuhs, J. L. Finney, C. Vettier, and D. V. Bliss, J. Chem. Phys. **81**, 3612 (1984).
[21] C. A. Tulk, R. E. Gagnon, H. Kiefte, and M. J. Clouter, J. Chem. Phys. **101**, 2350 (1994).
[22] V. G. Baonza, M. Caceres, and J. Nunez, Phys. Rev. B **51**, 28 (1995).